Translational Oncology
www.transonc.com

Volume 8 Number 3 June 2015 pp. 217–230 217

Pitfalls and Limitations of Diffusion-Weighted Magnetic Resonance Imaging in the Diagnosis of Urinary Bladder Cancer

Wei-Ching Lin[*,†] and Jeon-Hor Chen[‡,§]

*Department of Radiology, China Medical University Hospital; No. 2, Yuh-Der Rd, Taichung 40447, Taiwan (R.O.C.); [†]School of Medicine, China Medical University; No.91, Syueshih Rd, Taichung, 40402, Taiwan (R.O.C.); [‡]Department of Radiology, E-Da Hospital and I-Shou University; No.1, Yida Rd, Kaohsiung 82445, Taiwan; [§]Center for Functional Onco-Imaging, School of Medicine, University of California, Irvine; No. 164, Irvine Hall, Irvine, CA 92697, USA

Abstract

Adequately selecting a therapeutic approach for bladder cancer depends on accurate grading and staging. Substantial inaccuracy of clinical staging with bimanual examination, cystoscopy, and transurethral resection of bladder tumor has facilitated the increasing utility of magnetic resonance imaging to evaluate bladder cancer. Diffusion-weighted imaging (DWI) is a noninvasive functional magnetic resonance imaging technique. The high tissue contrast between cancers and surrounding tissues on DWI is derived from the difference of water molecules motion. DWI is potentially a useful tool for the detection, characterization, and staging of bladder cancers; it can also monitor posttreatment response and provide information on predicting tumor biophysical behaviors. Despite advancements in DWI techniques and the use of quantitative analysis to evaluate the apparent diffusion coefficient values, there are some inherent limitations in DWI interpretation related to relatively poor spatial resolution, lack of cancer specificity, and lack of standardized image acquisition protocols and data analysis procedures that restrict the application of DWI and reproducibility of apparent diffusion coefficient values. In addition, inadequate bladder distension, artifacts, thinness of bladder wall, cancerous mimickers of normal bladder wall and benign lesions, and variations in the manifestation of bladder cancer may interfere with diagnosis and monitoring of treatment. Recognition of these pitfalls and limitations can minimize their impact on image interpretation, and carefully applying the analyzed results and combining with pathologic grading and staging to clinical practice can contribute to the selection of an adequate treatment method to improve patient care.

Translational Oncology (2015) 8, 217–230

Introduction

Urinary bladder cancer is one of the most common urinary tract malignancies, causing notable morbidity and mortality [1,2]. The management and prognosis of bladder cancer are based on T staging, pathologic grading of the tumor, and the presence or absence of metastatic disease. Clinical staging of the primary tumor with bimanual examination, cystoscopy, and transurethral resection of bladder tumor (TURBT) is associated with an inaccuracy rate from 23% to 50% [3–7]. Therefore, obtaining an accurate imaging study is important to facilitate choosing optimal management methods.

Magnetic resonance imaging (MRI) is a feasible and reasonably accurate technique for the local staging of bladder cancer preferred over computed tomography (CT) [2] not only because MRI provides multiplanar images but also because the tissue contrast resolution is high. Furthermore, the application of functional images such as

Address all correspondence to: Jeon-Hor Chen, MD, Center for Functional Onco-Imaging, School of Medicine, University of California, Irvine, No. 164, Irvine Hall, Irvine, CA 92697, USA.
E-mail: jeonhc@uci.edu
Received 15 January 2015; Revised 6 April 2015; Accepted 9 April 2015

1936-5233/15
http://dx.doi.org/10.1016/j.tranon.2015.04.003

diffusion-weighted imaging (DWI) and dynamic contrast-enhanced imaging (DCE) to the anatomic images improves the accuracy of tumor detection and staging, and helps in monitoring posttherapy response and identifying recurrences [8–13].

DWI provides functional and structural information about biological tissues. It can be obtained rapidly and noninvasively without exposure to ionizing radiation and does not require gadolinium contrast administration. This is beneficial to a substantial group of bladder cancer patients who are allergic to contrast medium or who have renal dysfunction because it allows them to avoid contrast medium–induced nephrotoxicity and nephrogenic systemic fibrosis. DWI has played an important role in the multiparametric MRI and is a useful technique to increase the accuracy in detecting and evaluating the extent of bladder cancer [8–11,13]. In addition, it has also been applied to assess the biological behavior of bladder cancer. Apparent diffusion coefficient (ADC) value derived from DWI, which has been reported as a potential biomarker, could predict histopathological grading and reflect the aggressiveness of bladder cancer [14–18].

However, limitations exist, including a wide spectrum of cancer mimickers on DWI, intrinsic matters limiting the clinical applications of ADC values, inadequate patient preparation, presence of artifacts, and thinning of the bladder wall leading to inaccurate diagnosis, any of which could lead to under- or overstaging and impair the ability to determinate tumor aggressiveness. Moreover, difficult differentiation between benign lymph node and metastatic lymphadenopathy and interpretation of DWI in bone lesions also challenge the application of DWI to evaluate metastases. Although some studies have thoroughly reviewed the clinical use of DWI for bladder cancer assessment [19–21], pitfalls and limitations in the application of DWI to evaluate bladder cancer were not systemically reviewed. Full understanding of the limitations and careful avoidance of the pitfalls would promote more efficient use of DWI to assess bladder cancer.

Herein we described the biophysics of DWI and ADC, the histopathology of bladder cancer, the pitfalls and limitations in general utilization, and the clinical application of DWI for bladder cancer assessment based on our experiences and a review of the literature.

Biophysical Basis and General Limitations of DWI and ADC

Biophysical Basis of DWI

DWI is a functional imaging technique that depicts differences in the microscopic mobility of water molecules, called *Brownian motion*; this mobility depends on the integrity of cell membranes and the cellularity of the underlying tissue, thus reflecting biologic abnormalities. Advancement of imaging techniques, such as echo planar imaging, parallel imaging, multichannel coils, and high gradient amplitudes, has enabled the application of DWI in the abdomen and pelvis [22,23].

The movements of water molecules within some normal tissues, including neurological tissue, lymphatic tissue, bowel mucosa, testis, and endometrium, are restricted because these are highly cellular tissues that show persistently bright on DWI, even at high *b*-values. Pathologic lesions, such as tumor and infarction, have been reported to be associated with impeded water diffusion. Tumor tissue has high cellular density, high nuclear-cytoplasmic ratio, and high extracellular disorganization [22], causing restricted water diffusion leading to high signal intensity (SI) on DWI and reduced ADC value. Restricted water molecular movement in infarction is mainly related to cytotoxic edema. Water diffusion is also impeded in fibrosis and in the presence of highly viscous fluids such as abscess; thus, these conditions have the same SI on DWI and ADC as malignancy [24,25]. Lesions with a high fluid content have a strong T2 SI that may be carried onto the DWI to mimic or obscure cancer as a T2 shine-through effect. This pitfall may be avoided by referring to the ADC map and discloses its true diffusivity.

Quantifying the Degree of Water Diffusion

The ADC value is quantitative assessment of the SI changes of tissue as an increase of *b*-values. The calculation of ADC value is acquired via a diffusion equation that requires two or more *b*-values. The ADC map is a gray-scale display of the quantitative analysis of DWI. The "*b*-value" is proportional to the amplitude and duration of the applied gradient and the time interval between the paired gradients [22,23]. Changing the *b*-value alters the sensitivity to detect water diffusion. The SI of tissues on small *b*-values DWI incorporates both the slow diffusion component of thermally generated water mobility and the fast diffusion component that results from the mobility within the capillary network, whereas the fast diffusion component is restricted on higher *b*-values DWI. Increasing the *b*-value of DWI would get higher lesion-to-tissue contrast; however, this would decrease the signal-to-noise ratio and demonstrate greater image distortion. Moreover, as the *b*-value increased, the ADC value decreased [26] because of the exponential diffusion signal decay. ADC values were statistically higher using dual–*b*-value than multi–*b*-value DWI [13,25,27–30]. Few studies compared the application of DWI with different *b*-values in bladder cancer evaluation [26,31]; and no optimal *b*-values were recommended until recently, when it was recognized that further evaluation with extended variant *b*-values is needed.

General Limitations of ADC Applications

To obtain the ADC value, one can simply draw an optimal-sized region of interest (ROI), which avoids the partial volume effect on the ADC map. However, because of the heterogeneity of lesions and because ROI only appears on one or a few lesion-containing slices, ROI analysis may not reveal the condition of the whole lesion. Some researchers suggested that drawing a volume of interest (VOI) during analysis [17] has the potential for less operator dependence than traditional partial lesion ROI analysis, but to determinate accurate tumor margin during drawing a VOI is also a challenge. Because of poor anatomical details on DWI and ADC maps, it is necessary to combine T1-weighted imaging (T1WI) and T2-weighted imaging (T2WI) to evaluate lesion and to set ROI or VOI appropriately [21]. Moreover, the measurement of ADC value relies on the use of MRI systems, imaging sequences, and parameters that limit the reproducibility of the ADC value. For example, the ADC threshold for prostate cancer measured on fast spin echo DWI was 18% lower than echo planar imaging DWI [32]. The variation of ADC values measured at 1.5 and 3 T was up to 5% based on phantom studies [33] and with 4% to 9% variation of gray and white matter of the normal brain. And the variation was up to 8% when different coils were used on the same scanner [34]. In addition, ADC value is also susceptible to biological changes such as age and body temperature that cause interpatient variation [35,36]. Some investigators studied on normalized ADC by calculating the ADC ratio of lesion to surrounding normal tissues, such as urine within bladder. Assessment of normalized ADC would be an alternative method to standardize

the evaluation of ADC values. However, overlap of normalized ADC between low-grade tumors and high-grade tumors of the bladder does occur. Appropriate internal reference and reproducibility of normalized ADC between different observers and studies still need to be validated [37,38].

In summary, a wide spectrum of structures from normal tissue to malignancy showing high SI on DWI would cause difficulty in differential diagnosis and can lead to misdiagnosis. In addition, inherent variations in the equipment, biological changes of individual patients, and lack of standardized analytic methods will reduce the reliability of ADC comparisons between studies and limit the clinical application.

Pitfalls and Limitations from Inadequate Patient Preparation

Inadequate Bladder Distension

Optimal bladder distension is important in bladder cancer assessment. With a lack of bladder distention, small tumors will barely be visible secondary to detrusor muscle thickening. On the other hand, overdistension of the bladder may result in uncontrollable movements due to discomfort; and the thinness of bladder wall can decrease sensitivity for small lesions [39].

Adequate bladder distention can be achieved by instructing the patient to void 1 hour before imaging [8,31] or by instructing the patient to start drinking an adequate amount of water 30 minutes to 1 hour before the MRI study. In patients with a urethral catheter, a 250- to 400-mL sterile saline was used to distend the bladder [9,40]. However, it is difficult to obtain an adequately distended urinary bladder even by direct infusion of sterile saline via catheter placed into the bladder when the patient has a spastic and overactive bladder. This limits the application of MRI to evaluate bladder cancer in these patients, for example, in long-standing anuric uremia patients who frequently have bladder cancer. In addition, there are limitations in using MRI to evaluate bladder cancer in patients with an enlarged prostate, nerve dysfunction, and drug- or infection-related flaccid and overdistended bladder. These patients may require a catheter to drain excess urine and recheck on MRI localizer images to confirm that the bladder is adequate distended.

Gas-Produced Susceptibility Artifacts and Imaging Distortion

Susceptibility artifacts can occur next to gas-filled structures such as a gas-filled bowel and postprocedure gas bubbles within urinary bladder [41]. Susceptibility artifacts from gas in the small intestine, colon, and rectum around the urinary bladder can potentially cause image distortion with abnormally high SI of adjacent bladder walls on DWI that may be misrecognized as a flat-type cancer (Figure 1); and marked distortion can make cancer staging difficult (Figure 2). Gas bubbles within the bladder also result in artifacts at the air-wall interface that mimic malignancy (Figure 3). The common causes of gas retained in the urinary bladder include the aftereffects of cystoscopy or an indwelling Foley catheter that MRI is not recommended following these procedures. These gas produced susceptibility artifacts are increased while increasing the main magnetic field strength and are approximately twice as large in terms of volume at 3.0 T as at standard 1.5-T MRI [42]. It is believed that some important findings may be obscured by these enlarged susceptibility artifacts at 3.0-T MRI but may be visualized at standard 1.5-T MRI [41] because DWI is a gradient echo image that will amplify these susceptibility artifacts and cause obvious image distortion than T2WI. Identifying these susceptibility artifacts on DWI and correlating them to anatomic images will help in obtaining accurate diagnosis and staging.

Pitfalls and Limitations in Detection of Bladder Cancer

Causes of Underdetection

High–*b*-value DWI is almost always used to detect lesion when evaluating cancer. The maximal *b*-value used to evaluate various organs in the abdomen and pelvis ranges from 500 to 1000 s/mm^2. Benign prostate parenchyma may retain mild high SI, and some focal lesions will sink in this high-SI parenchyma due to the impaction of T2 component on DWI using this range of *b*-values [43]. Similarly, urine may persistently show mild high SI in patients with bladder cancer that will also lead to underdetection of intraluminal tumor. Carefully comparing with ADC map, T2WI, and DCE or use of an ultrahigh–*b*-value DWI would improve tumor recognition and differentiation [31,44,45].

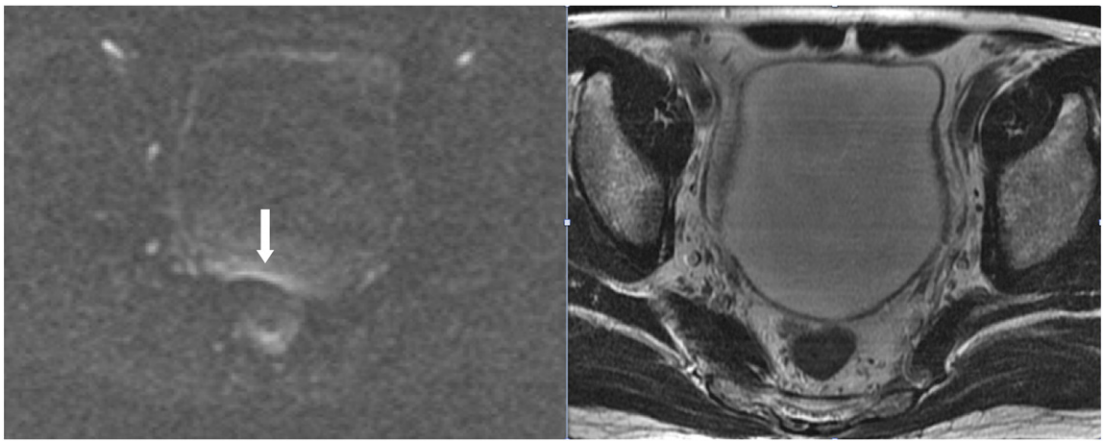

Figure 1. A 61-year-old man suffered from gross hematuria due to bladder cancer. Rectal gas causes a band-like high-SI artifact on the posterior bladder wall (*arrow*) that mimics a flat-type cancer on DWI (*left*). No obvious SI change is observed on T2WI (*right*) and DCE (*not shown*); cystoscopy revealed no tumor in this area of bladder.

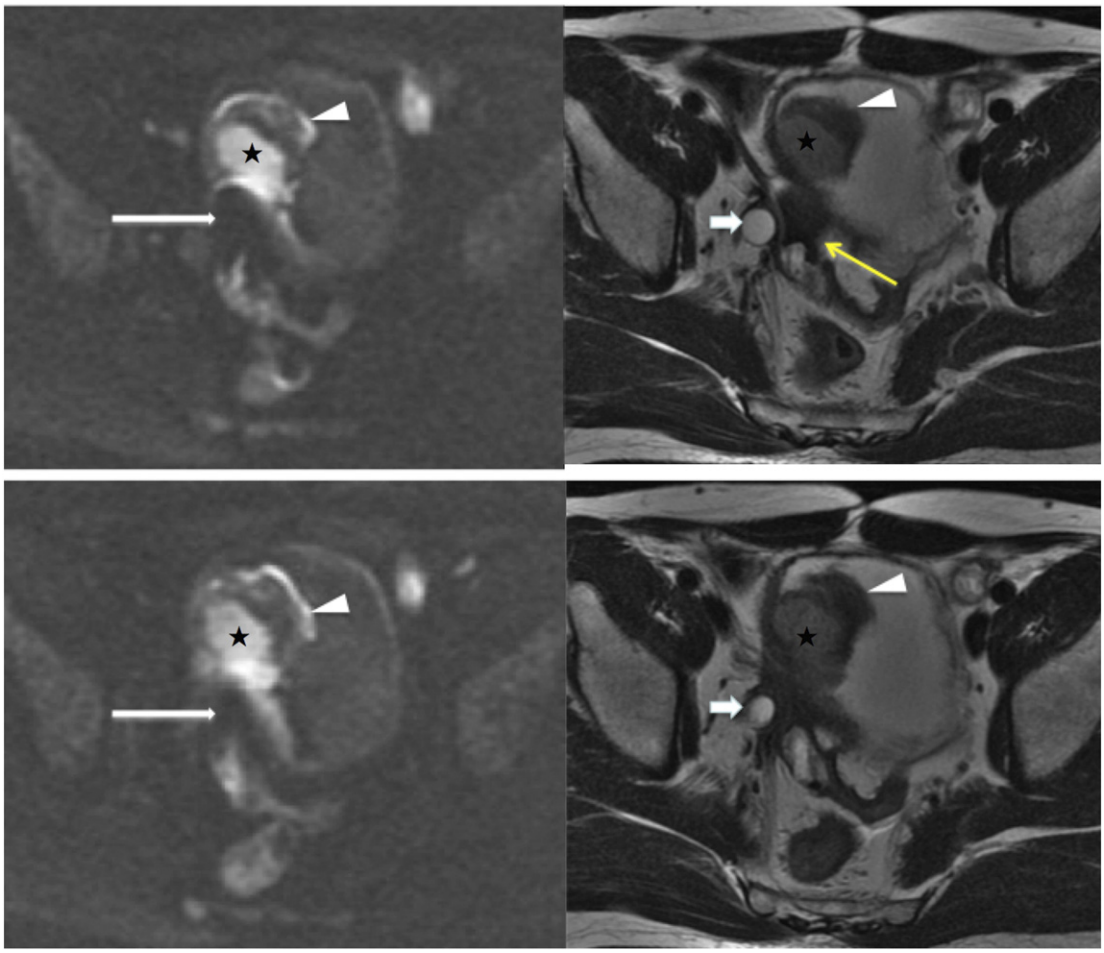

Figure 2. A 60-year-old man who had bladder cancer with right ureter, prostate, and bilateral seminal vesicle invasion underwent MRI following chemotherapy for preoperative restaging. A prominent susceptibility artifact (*long white arrows*) adjacent to the tumor base (*stars*) due to gas in the sigmoid colon is noted on two consecutive sections of DWI (*left*), and this interferes with the evaluation of tumor invasion. The gas and fluid contained sigmoid colon (*yellow arrow*) and can be well recognized on T2WI (*right*). Some hypointense lesions can be seen around the dilated right ureter (*short arrows*) and bladder wall at tumor base; however, these images cannot differentiate residual cancer from scar tissue. Note that a blood clot on the tumor surface shows low SI with a high-SI rim on DWI and low SI on T2WI (*arrowheads*).

Bladder cancers generally show higher SI than surrounding tissues on high–*b*-value DWI [25,28,30]. Several studies had reported high sensitivity, specificity, and accuracy for identifying bladder cancers as 90% to 98%, 85% to 93%, and 89% to 97%, respectively [9,26,29,40,46]. Nevertheless, because of poor spatial resolution of DWI and insufficiency of tissue contrast between small tumors and normal bladder wall, bladder cancer less than 1 cm may be missed on DWI [9,14,26,40]. Similarly, DWI is also not reliable for the assessment of carcinoma in situ that is generally excluded out of studies [14,17,46].

Blood Clots Effects

Occasionally, high-SI blood clots on DWI accompany bladder cancer. These blood clots may also cause local image distortion due to magnetic susceptibility effects [47]. The SI of blood clots on DWI is complex and is related to the relative amount of different hemorrhagic products and the pulse sequence used (Table 1) [42,47,48]. Oxyhemoglobin shows hyperintensity on DWI and has a low ADC value, indicating the relative restriction of water movement inside the red blood cells [42,48]. Increased water mobility of extracellular methemoglobin eliminates the inhomogeneous susceptibility effect and results in a higher ADC value [42,48]; however, prolonging the T2 component of the fluid with extracellular methemoglobin shows hyperintensity on DWI. Other blood clot components, including deoxyhemoglobin, intracellular methemoglobin, and hemosiderin, show low SI on DWI because of magnetic susceptibility effects; and ADC values cannot be reliably calculated for these hemorrhage products because they have very low SI on T2WI [49]. Overall, these high-SI or low-SI blood clots can potentially mask an underlying small tumor or lead to false-positive diagnosis for tumors (Figures 4–6).

Pitfalls and Limitations in Characterization of Bladder Cancer

Bladder Cancer Mimickers

The urachus has some variability in the terminus of the lower end [50] that causes variable SI in the apex of the bladder wall. The urachal remnant is a fibroepithelial canal; and when the intravesical segment of the urachal remnant has high SI on DWI, it can also be confused with bladder cancer (Figure 7).

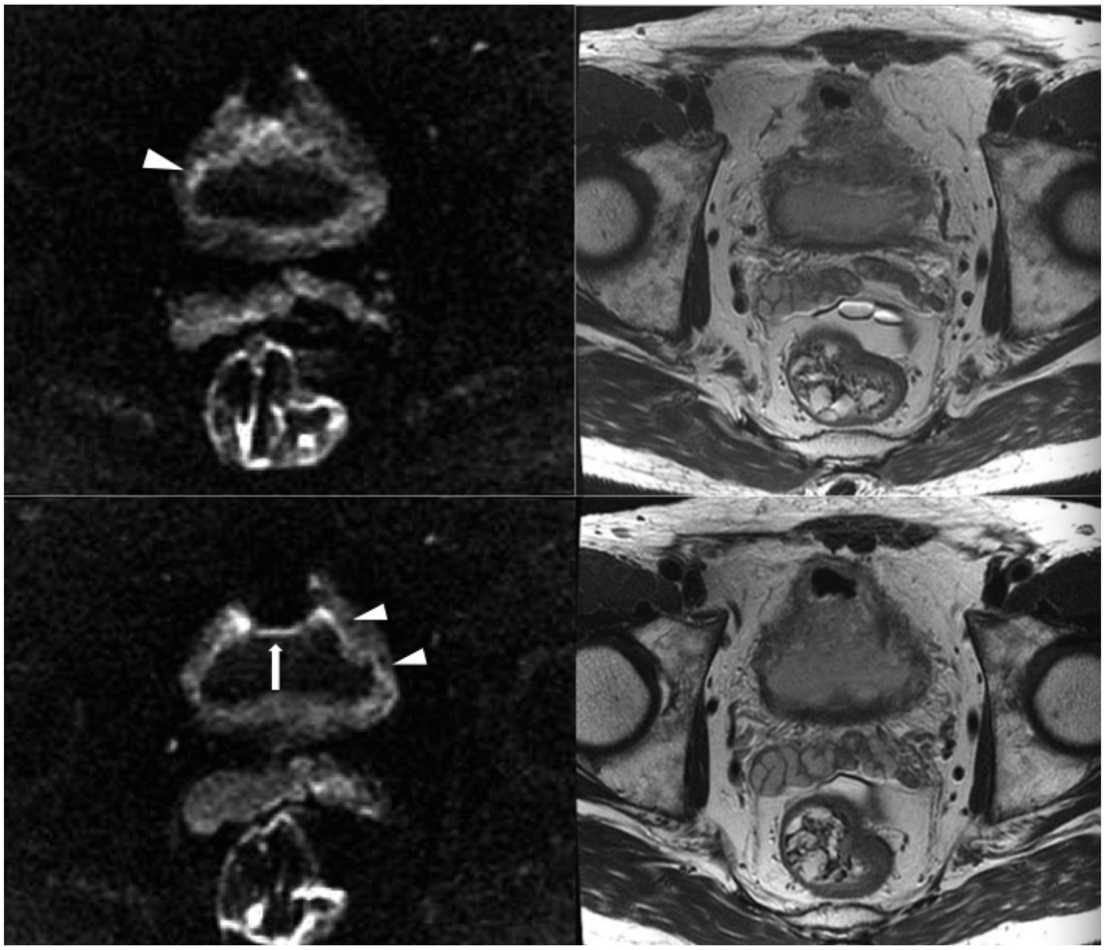

Figure 3. A 70-year-old man with a history of carcinoma in situ of the bladder after intravesicle immunotherapy with bacillus Calmette-Guerin and a history of prostate carcinoma presented with hematuria. Diffuse bladder wall thickening with long segmental linear mild high SI (*arrowheads*) in the inner portion of thick bladder wall on DWI (*left*) mimics an infiltrative tumor and shows no obvious SI change on T2WI (*right*). However, pathology of transurethral bladder resection specimens demonstrated chronic inflammation with focal granulomatous inflammation and no malignancy. Note that gas in the anterior portion of the bladder caused a high-SI artifact on the anterior bladder wall (*arrow*).

Inflammatory processes of the bladder wall such as interstitial cystitis, cystitis cystica, eosinophilic cystitis, polypoid cystitis (uroepithelial papilloma), and post-TURBT inflammation, especially at early post-TURBT phase, have been reported to show high SI on DWI and ADC maps, which could be differentiated from cancer, due to the edematous tissue, inflammation, or fibrosis [12,13,26]. However, sometimes they might also cause decreased ADC values that would be misinterpreted as cancer [12,13,26]. Other granulomatous or nongranulomatous chronic inflammatory processes with or without fibrosis and benign wall thickening secondary to benign prostatic hyperplasia may also show high signal changes on DWI [12,13,29]. These inflammatory processes can be diffuse, occupying the whole bladder (Figure 3), or appear as a focal lesion within the bladder (Figure 8). They also showed low SI on T2WI and early enhancement on DCE that mimics the image findings of malignancy on MRI. In addition, clinical presentation and cystoscopy of these inflammatory processes can occasionally mimic cancer and may sometimes coexist with malignancy; for these reasons, biopsy is always recommended.

Table 1. Signal Intensities of Different Stages of Hematoma Demonstrated on MR Images

	T1WI	T2WI	DWI	ADC map
Intracellular oxyhemoglobin	Isointense	Hyperintense	Hyperintense	Hypointense
Intracellular deoxyhemoglobin	Isointense	Hypointense	Hypointense	Hypointense
Intracellular methemoglobin	Hyperintense	Hypointense	Hypointense	Hypointense
Extracellular methemoglobin	Hyperintense	Hyperintense	Hyperintense	Hyperintense
Intracellular hemosiderin	Hypointense	Hypointense	Hypointense	Hypointense

Although several studies have shown that ADC values of bladder malignancy are lower than those of benign bladder lesions and normal bladder wall, there is substantial overlapping between malignancy and benignancy [8,13,22,25,26,28–30,40,51]. Lack of a conclusive cutoff ADC value from these studies would limit the application of ADC value in differentiating malignancy from benign lesion and normal bladder wall.

Limitations in Discriminating the Histopathological Subgroups of Bladder Cancer

Cancers in bladder can be primary, metastases, or invasive tumors from adjacent malignancies. Ninety percent of bladder cancers are transitional cell carcinoma (TCC); and the other 10% are squamous cell carcinoma, adenocarcinoma, sarcoma, small cell carcinoma,

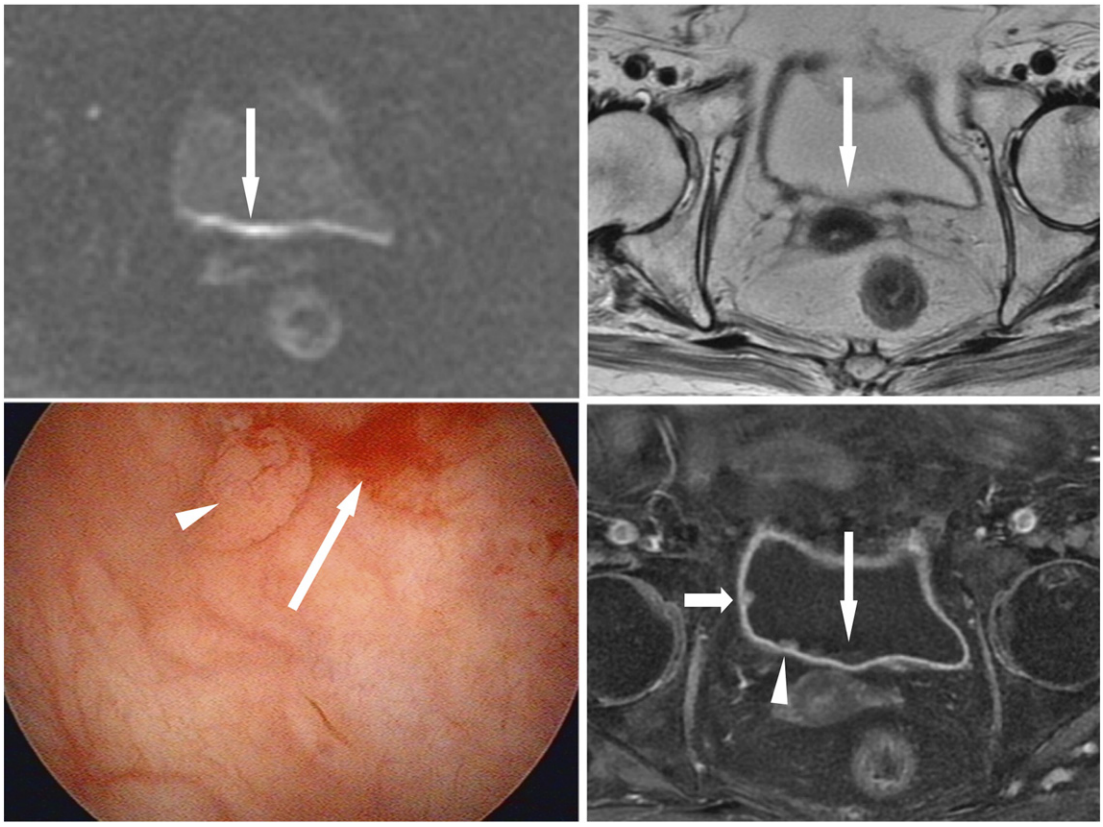

Figure 4. An 86-year-old woman presented with gross hematuria due to bladder cancer. A long linear high SI (*long arrows*) located at the posterior wall of the bladder on DWI (*top left*) mimics a flat-type cancer. It shows isointensity with urine on T2WI (*top right*) and mild high SI with urine without enhancement on DCE (*bottom right*) corresponding to the SI of a blood clot. A small tumor beside the right ureteral orifice (*arrowheads*) is noted on DCE, but it is difficult to distinguish the SI of the tumor from that of the blood clot on DWI. A small tumor (*short arrow*) in the right lateral wall is also noted on DCE but is unrecognized on DWI and T2WI. Cystoscopy (*bottom left*) confirms these findings.

metastases, and invasive tumors from other pelvic malignancies. A variety of bladder cancers presumably show high SI on DWI and have low ADC values [8,9,26,30,40]. Because of the rarity of non-TCC, there is limited literature focus on distinguishing TCC from non-TCC of bladder on DWI. Daggulli et al., [26] found that the ADC values of TCC were significantly higher than those of squamous cell carcinoma, but El-Assmy et al., [30] did not. Generally, non-TCC of bladder is reported to be more aggressive and usually extends beyond the bladder wall, and is usually larger than TCC of the bladder at the initial time of diagnosis [52–54].

TCCs are categorized as high- or low-grade tumors based on how abnormal the cells look under microscopy. Some researchers reported that the mean ADC values of high-grade cancers (0.69-0.92 $\times 10^{-3}$ mm^2/s) were lower than those of lower-grade cancers (0.92-1.6 $\times 10^{-3}$ mm^2/s)

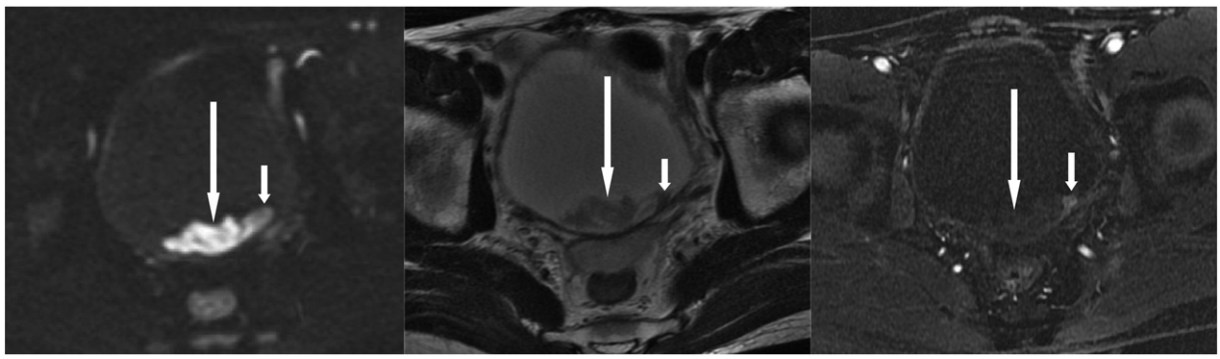

Figure 5. A 41-year-old man presented with gross hematuria due to bladder cancer. Cystoscopy showed a bladder mass. Axial sections of DWI (*left*) and T2WI (*middle*) reveal a hyperintense lobulated contour mass (*long arrows*) in the depending portion of the bladder; and DCE (*right*) reveals a small early enhanced nodule within this mass, indicating that the tumor (*short arrows*) is hidden within the blood clot (*long arrows*).

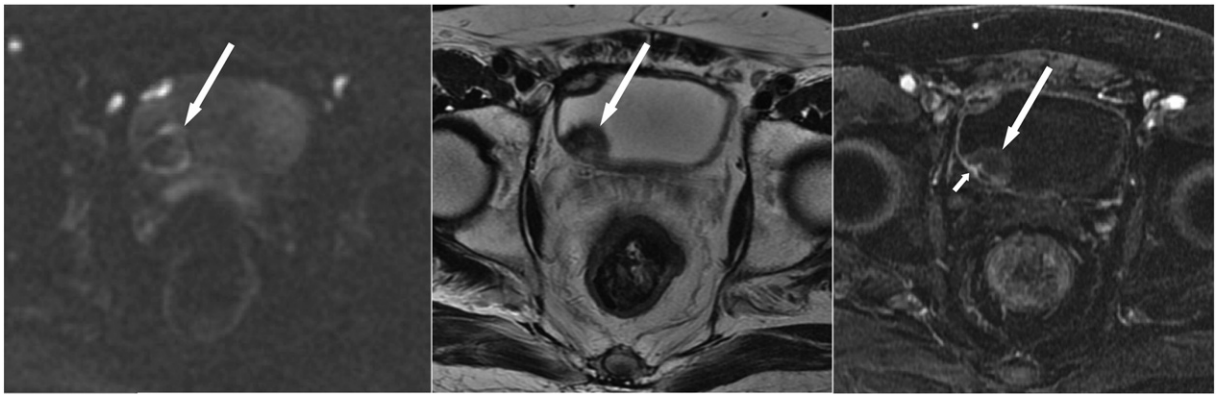

Figure 6. An 88-year-old man was admitted because of gross hematuria. Axial sections of DWI (*left*), T2WI (*middle*), and DCE (*right*) reveal a nodule in the right posterolateral wall showing low SI with a high-SI rim (*long arrows*) on DWI, heterogeneous SI on T2WI, and no enhancement on DCE, indicating a blood clot. In addition, a small enhanced tumor (*short arrow*) proven to be cancer and hidden within the blood clot is only well demonstrated by DCE.

[8,13,26,46]. However, the ADC values overlap between high-grade and low-grade tumors and between low-grade tumors and some benign lesions [13]. It is essential to note that ADC value is a quantitative analysis, the cutoff point of ADC value is not providing a "yes" or "no" answer, and it gives only a gradient of clinical impression. This limits the application of ADC to distinguish a high-grade tumor from low-grade tumor or distinguish low-grade tumor from a focal cystitis, or find a low-grade tumor out of diffuse cystitis.

Pitfalls and Limitations in Staging of Bladder Cancer

Local Staging

It is important to distinguish muscle-invasive tumors from non–muscle-invasive tumors because the management is varied. Utility of divergent staging criteria, relatively poor spatial resolution of DWI, thinness of the muscle layer, and the different appearance of cancer may cause varying accuracy of DWI in staging bladder cancer. It was reported that the accuracy of using DWI alone to discriminate muscle-invasive tumors from non–muscle-invasive tumors ranges from 63.6% to 92% [9,46,55,56].

Staging of bladder cancer by DWI alone is in general unsatisfactory [46], although a study revealed high accuracy of staging bladder cancer with the combination of DWI and T2WI [8]. Staging a tumor with a stalk showing imaging of "inchworm sign" not only is seen in stage Ta or stage T1 tumors but also can be seen in stage T2 tumors [46,57,58]. It is occasionally unable to determinate if the tumor margin is smooth on DWI, which makes the correct categorization of the tumor as stage T2 or stage T3 difficult [8]. Moreover, frequent loss of normal signals of the thin muscle layer on DWI at some areas of bladder wall, such as the junction of the lateroposterior wall, also contributes to inaccurate staging (Figures 9–11). High-resolution oblique T2WI perpendicular to the wall at tumor base allows avoiding the partial volume effect of adjacent tissues on bladder wall. This improves the evaluation of the relationship of high-SI tumor to the low SI of muscle layer [59]. However, oblique DWI still cannot be optimized to achieve enough signal-to-noise ratio and may cause more image distortion.

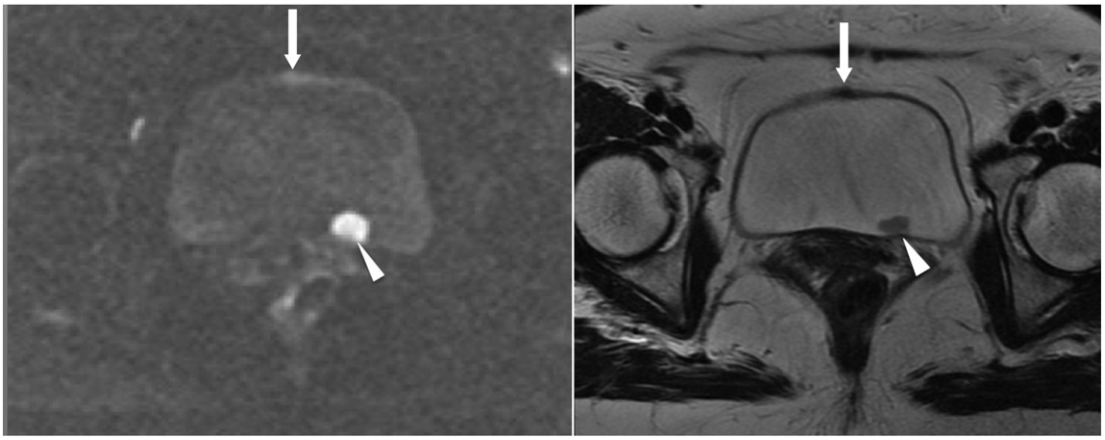

Figure 7. A 54-year-old woman had painless gross hematuria due to bladder cancer. Axial section of DWI (*left*) reveals a focal lesion (*arrow*) with SI higher than the normal bladder wall but lower than the high-grade carcinoma (*arrowhead*) in the left posterior wall on DWI. The focal lesion (*arrow*) appears hypointense on T2WI (*right*), and its SI is also lower than the high-grade carcinoma (*arrowhead*). This suspicious lesion corresponds to the urachal remnant and should not be mistaken as a low-grade tumor.

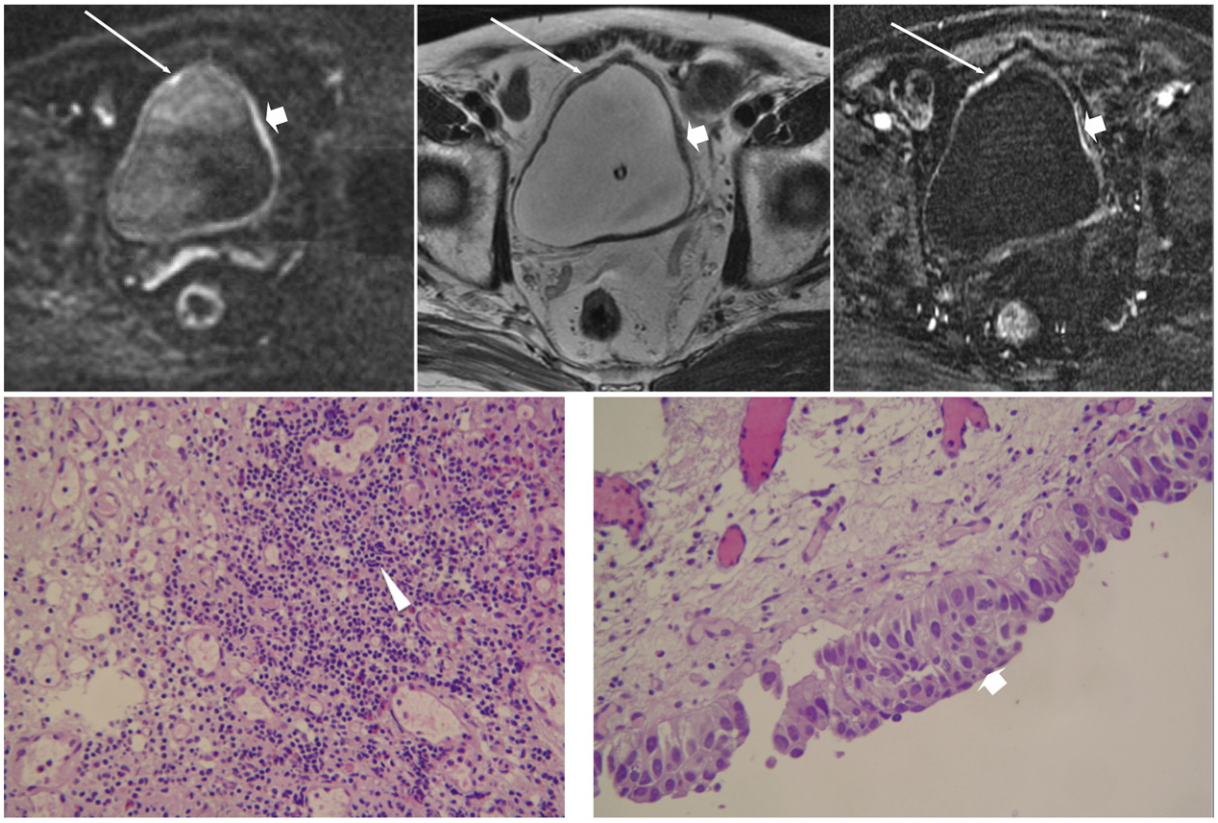

Figure 8. A 79-year-old man underwent an imaging survey because of microscopic hematuria. Axial sections of DWI (*top left*), T2WI (*top middle*), and DCE (*top right*) reveal two lesions of similar SI, one in the right anterior dome (*long arrows*) and the other in the left lateral wall (*short arrows*), showing high SI on DWI, early enhancement on DCE, and only slight wall thickening without change in signal on T2WI. The pathology image of the right anterior dome lesion (*bottom left*) demonstrates chronic inflammation of the bladder mucosa with increased lymphocytic infiltration (*arrowhead*), and the result for the left lateral wall lesion (*bottom right*) shows carcinoma in situ (*short arrow*).

Several studies reported high accuracy of MRI for tumor staging; however, these MRIs were performed before TURBT [8,9,56]. Post TURBT would induce inflammation, and the inflammation is more prominent at early post-TURBT phase. If MRI is performed early after TURBT, it may result in overstaging and even misinterpretation of inflammation for disease. Sometimes, this post-TURBT inflammation would also miss small tumors, thus understaging the disease [12].

Infiltrative scattered tumors may not generate enough high signals on DWI to be discriminated from normal bladder that can be underdetected and lead to understaging (Figure 12). Furthermore, the diagnosis of metastasis or invasion to some pelvic structures such as testis, penis, seminal vesicle, and endometrium from bladder cancer should be carefully made because these structures physiologically show high SI on DWI. Therefore, when staging bladder cancer, it is always needed to combine DWI with anatomic images and ADC values rather than using DWI alone.

Lymph Node Metastasis

The sensitivities and specificities of lymph node detection on routine MRI combined with DWI for bladder cancer were 76% to 79% and 79% to 89%, respectively, which were higher than those of conventional CT and MRI alone. But the accuracy remains unsatisfactory, even with the combination of DWI and routine MRI with the use of ultra-small superparamagnetic particles of iron oxide [60–64]. A significant number of patients staged as N0 with unexpected microscopic lymph node metastasis are found after radical cystectomy and pelvic lymph node dissection [65–68]. The major limitation arises from failure to identify small metastatic lymph nodes due to the limited spatial resolution of DWI; lack of anatomical structures especially in the high–*b*-value images; artifacts from adjacent bowel gas, motion, metal surgical clips, and pulsatile vessels [69,70]; and a tiny component of metastases in lymph nodes unable to raise enough tissue contrast [61–64]. Furthermore, it is important to note that normal lymph nodes may show intermediate to high SI on DWI due to the high cellularity of lymphoid tissue [19]. Some studies have investigated the utility of ADC value to discriminate metastatic from benign lymph nodes. They found significantly lower mean ADC values in malignant lymph nodes than benign lymph nodes [61,63]. However, ADC values overlap between benign and malignant nodes [61,63] because some benign processes of lymph nodes, such as inflammation, sinus histiocytosis, fibrosis, follicular hyperplasia, and lipomatosis, also cause restriction of water diffusion. In addition, partial volume effect, affecting the measurement of the ADC values of these small lymph nodes, also leads to the inconsistent results on the application of ADC [61–64].

Because of high false-negative rate in using DWI to detect metastatic lymph nodes, an indicated extended pelvic lymph node dissection cannot be prohibited by negative study on DWI, even combined with the use of ultra-small superparamagnetic particles of iron oxide [61–64].

Bone Metastasis

Abnormal high SI of pelvic bones found on DWI in routine staging MRI is not rare, and 27% of these findings are bony metastasis [71].

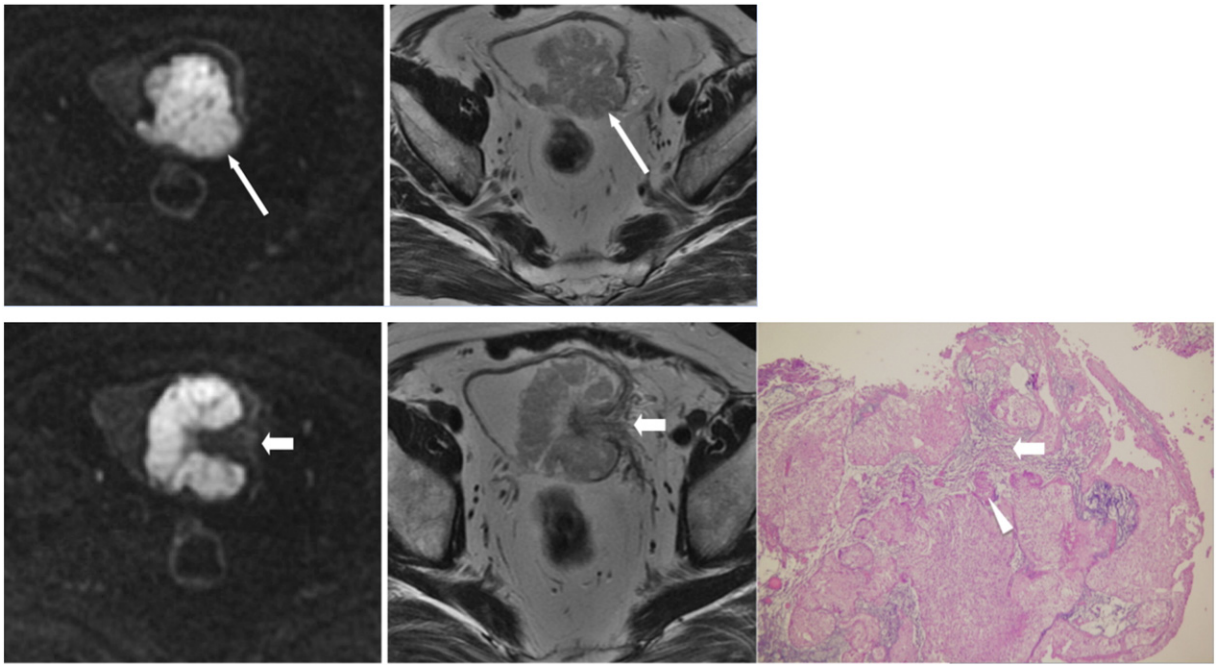

Figure 9. A 63-year-old man presented with gross hematuria due to bladder cancer. Axial section images of DWI (*top left*) and T2WI (*top right*) taken from the cephalic portion of the tumor reveal that the tumor extends out of the bladder wall with smooth contour (*long arrows*), indicating at least stage T2. Axial sections of DWI (*bottom left*) and T2WI (*bottom middle*) of the central portion of the tumor show a submucosal stalk (*short arrows*). Final pathology (*bottom right*) shows that the tumor nests (*arrowheads*) only invade the lamina propria (short arrow) and not the muscle layer (*not shown*), indicating stage T1.

The interpretation of DWI in bone lesions differs from that in soft tissue lesions because the relationship between cellularity and ADC values in bone marrow is nonlinear [72]. The reduced water content, the large-sized fat cells, the hydrophobic nature of fat, and poor perfusion contribute to low SI on DWI and ADC values of yellow bone marrow. Increased cellularity, abundant water content, and rich perfusion of red marrow, like cancer, show increased SI on DWI but paradoxically high ADC values [73,74]. Generally, the SI of bone marrow varies; and normal adult bone marrow pattern, that is, the distribution of red and yellow marrow, is established by age 25 years. The changing distribution of red and yellow marrows is dependent on patients' age, sex, and underlying medical conditions that sequentially affect the SI of bone marrow on DWI [72]. These limit the application of DWI in detection of bony metastases and characterization of bone lesions.

Pitfalls and limitations on visual assessment of bony metastases. Bony metastases generally show high SI on high–*b*-value DWI. However, the ability to detect these metastases is dependent on the cellularity and cell size of the tumor, the background bone marrow, the location of metastases, and treatment status [75]. DWI is better at detecting bony metastases from small cell cancers such as myeloma, lymphoma, and neuroendocrine tumors than TCC of bladder [76,77]. Early mild metastatic cancer cell infiltration or hyperplasia of background bone marrow would cause a false-negative finding on DWI [78]. In addition, relatively increased cellularity in bone marrow is observed in bladder cancer patients who are smokers, have chronic heart failure, and are

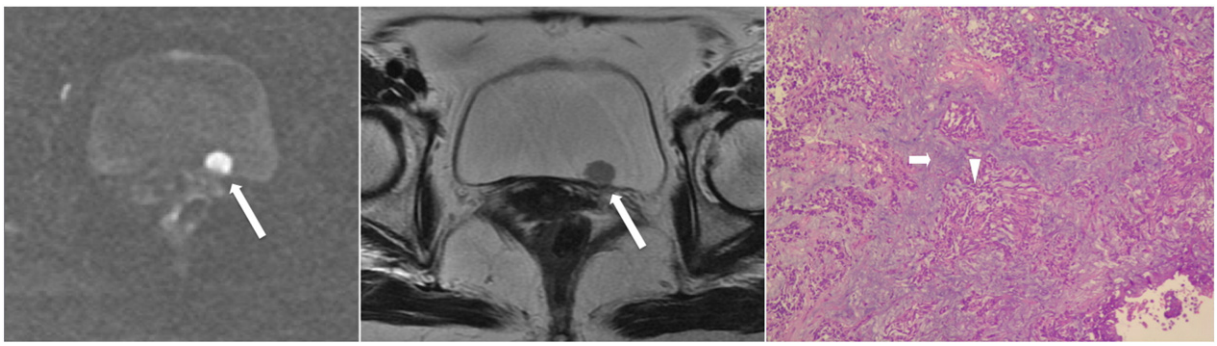

Figure 10. A 54-year-old woman had painless gross hematuria due to bladder cancer. Axial sections of DWI (*left*) and T2WI (*middle*) show a tumor (*long arrows*) in the left posterior wall with discontinuity of hypointense muscle layer, indicating stage T2. However, pathology (*right*) reveals high-grade tumor (*arrowhead*) infiltration in the lamina propria (*short arrow*) but not in the muscle layer, indicating stage T1.

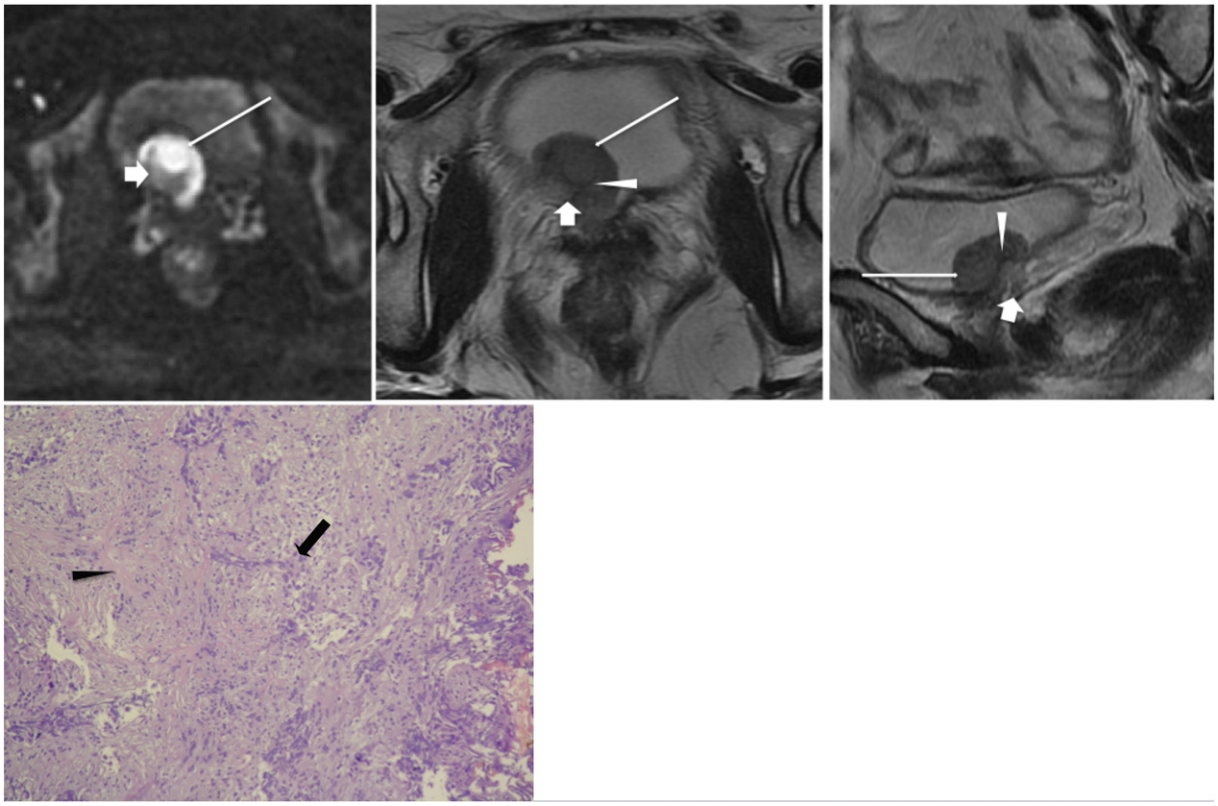

Figure 11. A 53-year-old woman had gross hematuria due to bladder cancer. Axial sections of DWI (*top left*) and T2WI (*top middle*) and sagittal section of T2WI (*top right*) reveal a broad-base tumor (*long white arrows*) located over the right bladder neck and right bladder base. In addition to a hyperintense tumor area found on DWI, a crescent moon–shaped hypointense area within the central base region is also shown on DWI; and it shows high SI on T2WI (*short white arrows*), which mimics a thickened submucosa. Pathology (*bottom*) shows that the tumor (*black arrow*) infiltrates the muscle layer (*black arrowhead*) without extending into the perivesical fat, indicating stage T2. Retrospective review of the DWI and T2WI shows that a thin, curvilinear low SI (white *arrowheads*) could be found between the base of the tumor and the crescent moon–shaped lesion on T2WI, corresponding to the muscle layer; the signal of the muscle layer on DWI could not be identified in the tumor region. The crescent moon–shaped lesion is perivesical fat attracted into the tumor implanted region, not the thickened submucosa.

treated with hematopoietic growth factors such as granulocyte colony-stimulating factors [73,78]. These patients may show increased SI on DWI, which could not only hide metastatic cancer cell infiltration but also be mistaken as false-positive diagnosis. DWI is of limited value in detecting metastases in some bony regions such as at anterior ribs and sternum due to motion, and in the skull base due to susceptibility artifacts. Sclerotic or posttreated bony metastases are more difficult to detect on DWI than diffuse, highly cellular infiltrative lytic bony metastases because of the lower water and cellular content. Rather, T1WI showed the best ability to detect sclerotic bone metastases against the surrounding tissue [70].

Some benign bone conditions, such as fractures, osteoarthritis, infection, intraosseous hemangioma, giant cell tumor of bone, and treatment-induced bone marrow edema would lead to a false-positive diagnosis on DWI because of the T2 shine-through effect [79–81]. Susceptibility artifacts resulting from various factors, including metallic prostheses, air of adjacent bowel loops, and fat-water interfaces, may also cause false-positive findings [79].

Limitations of applying ADC to evaluate bony metastases. Because the diffusion coefficient of fat is approximately two orders of magnitude lower than that of water and there are abundant fatty components in the normal marrow, lipid contamination within the ROI of bony metastases will lower the measured ADC value [82,83]. Moreover, ADC values overlap between malignancy and benign bone lesions, thus limiting the application in the discrimination of bony metastasis from bladder cancer to primary bony malignancy and benignancy [84–87].

In summary, because of many aforementioned factors, the interpretation of DWI in bone lesions differs from that in soft tissue lesions. To achieve accurate diagnosis, careful comparison of findings on DWI with anatomic images of MRI, conventional radiograph, positron emission tomography/CT, and bone scan, and correlation with clinical findings, should be taken.

Pitfalls and Limitations in Predicting the Aggressiveness of Bladder Cancer

Some studies showed that ADC value could predict bladder cancer aggressiveness because lower ADC value or kurtosis is associated with post-TURBT recurrence in non–muscle-invasive disease [88], tumor with lymph node and distant metastases [17,89], and tumor response to chemoradiation therapy [90]. The reason that more aggressive bladder cancer has a lower ADC value is not well recognized but is presumed to be associated not only with morphological tumor features such as higher cellularity, tissue disorganization, and decreased extracellular space but also with biologic properties such as strength of intercellular adhesion of primary tumor from which

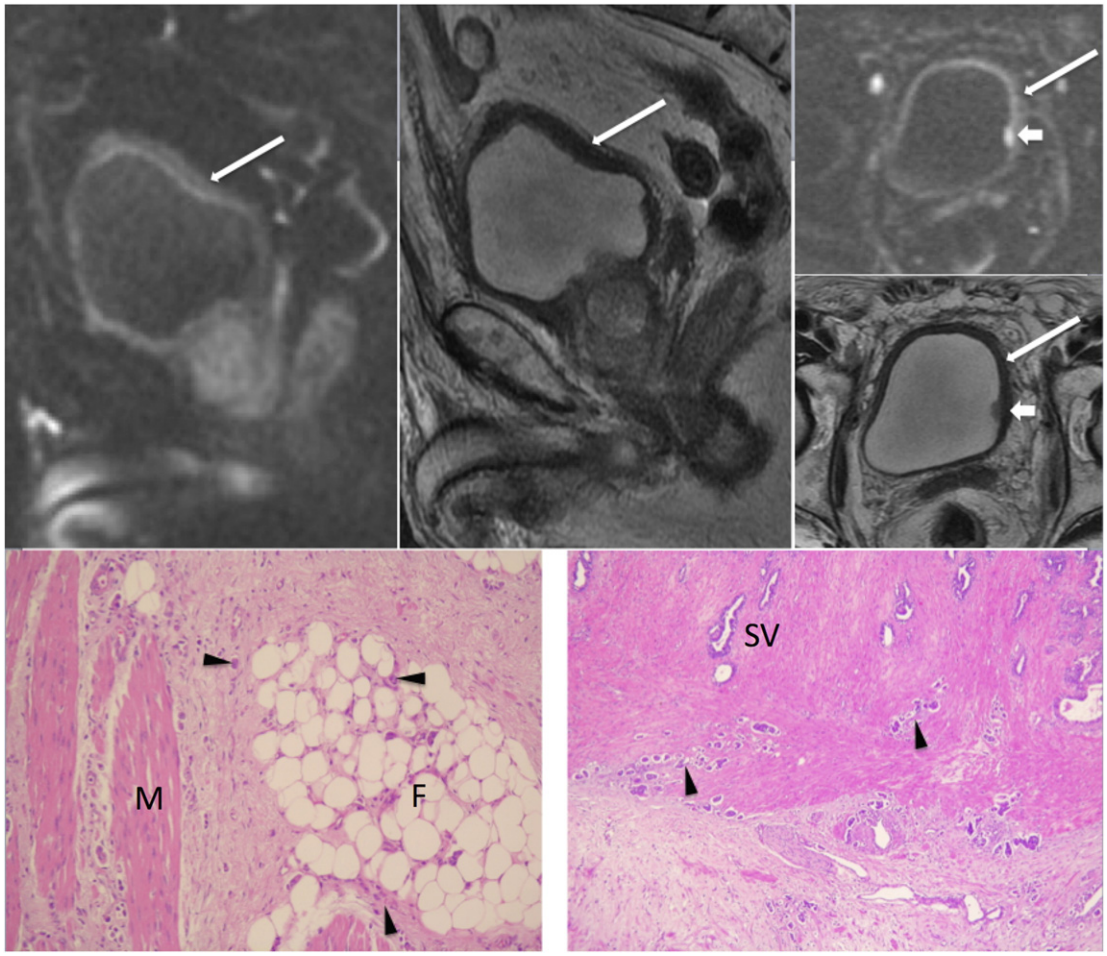

Figure 12. An 82-year-old man presented with hematuria due to bladder cancer. DWI in sagittal and axial views (*top left and top right upper*) reveals some band-like hyperintensities (*long arrows*) along the urinary bladder wall with one small hyperintense lesion (*short arrows*) in the left lateral wall. T2WI in sagittal and axial views (*top middle and top right lower*) only shows the focal lesion in the left lateral wall and a thick bladder wall corresponding to the area of mild high SI on DWI. There is no evidence of extravesical or seminal vesicle invasion on MRI. Atrophic bilateral seminal vesicles are also noted. The patient underwent cystoscopy and transurethral resection of the bladder tumor, and demonstrated invasion of multiple infiltrative high-grade tumors in the left lateral wall, trigone, base, and left posterior wall extending to the right posterior and lateral wall (*not shown*). Radical cystoprostatectomy with bilateral pelvic node dissection and ileal conduit diversion was thus performed. Pathology reveals diffuse high-grade infiltrative carcinoma (*arrowheads*) with invasion through the muscularis propria (*M; bottom left*) into the perivesical soft tissue (*F; bottom left*) and bilateral seminal vesicles (*SV; bottom right*) with lymph node metastasis (*not shown*).

recurrence arises [88] and molecule profile that involves apoptosis [91], cell cycle, and proliferative regulation [14,16]. However, these findings were based on limited studies with low patient numbers [14,16,17,88–90] or biased patients' selection [14,17,88,89]. Contradictory findings also exist [17,89].

Studies have noted that several proliferative regulators, such as Ki-67, p53, p21, pRB/p16, HER2, p27, and cyclin E1, can predict patients with localized bladder cancer who are at risk of disease progression and recurrence. This is due to the presence of occult metastases at diagnosis [14,16,92–94]. Therefore, these patients would benefit from systemic adjuvant chemotherapy. To obtain these biomarkers requires invasive tissue sampling and human interaction in selecting representative slides for analysis. Acquiring ADC value is, however, noninvasive. However, there are only limited studies performed to correlate DWI-derived ADC value with these biomarkers. These studies showed that ADC values correlate with prognostic factors of ki-67–, p53-, and p21-positive cells on histopathology [14,16]; but ADC merely provides an incremental prognostic value and cannot replace these traditional prognostic markers [16]. Because DWI method is different among the studies, one of the future directions of MRI/DWI applied on bladder cancer is to correlate standardized ADC measurements with the cell cycle and proliferative regulators; and the results can potentially be used to predict cancer aggressiveness.

Overall, despite some encouraging results, direct application of ADC values to replace other prognostic biomarkers is not recommended. Further studies with larger patient numbers using standardized ADC value measurements are necessary to verify the ability of ADC value to predict cancer aggressiveness.

Pitfalls and Limitations in Monitoring Posttreatment Bladder Cancer

Although DWI has a superior specificity and accuracy to T2WI or DCE, all of them have similar low sensitivity of 43% to 57% [95].

There is also a substantial overlap of ADC values between recurrent tumors and the surrounding bladder wall that may be attributable to the inflammatory reaction from previous TURBT [96]. Currently, DWI still cannot replace cystoscopy to identify posttreatment recurrence because of its limitations in discriminating posttherapeutic inflammatory changes and fibrosis from small or microscopic viable tumors [12,95,96].

Conclusions

DWI is a noninvasive functional imaging technique and has been increasingly used as part of multiparametric MRI to evaluate bladder cancer. It provides not only qualitative information to diagnosis of bladder cancer but also quantitative analysis to predict the clinical aggressiveness. Despite its potential utility, there are limitations and pitfalls in clinical application of DWI; thus, pathology and clinical findings should always be taken into account when interpreting the MR images. Recognizing the inherent limitations, imaging artifacts, and cancer mimickers of DWI, and variant manifestations of bladder cancer on DWI with careful interpretation, and combining with pathologic and clinical findings could improve the diagnostic accuracy that facilitates the selection of an appropriate treatment method for a patient.

Acknowledgements

We thank Han Chang, MD (Department of Pathology, China Medical University Hospital), and Chao-Hsiang Chang, MD (Department of Urology, China Medical University Hospital), for their help with figures of pathology and cystoscopy for this article.

References

[1] Jacobs BL, Lee CT, and Montie JE (2010). Bladder cancer in 2010: how far have we come? *CA Cancer J Clin* **60**, 244–272.
[2] Siegel R, Naishadham D, and Jemal A (2013). Cancer statistics, 2013. *CA Cancer J Clin* **63**, 11–30.
[3] MacVicar AD (2000). Bladder cancer staging. *BJU Int* **86**(Suppl. 1), 111–122.
[4] Stein JP, Lieskovsky G, Cote R, Groshen S, Feng AC, Boyd S, Skinner E, Bochner B, Thangathurai D, and Mikhail M, et al (2001). Radical cystectomy in the treatment of invasive bladder cancer: long-term results in 1,054 patients. *J Clin Oncol* **19**, 666–675.
[5] Dutta SC, Smith Jr JA, Shappell SB, Coffey CS, Chang SS, and Cookson MS (2001). Clinical under staging of high risk nonmuscle invasive urothelial carcinoma treated with radical cystectomy. *J Urol* **166**, 490–493.
[6] Ficarra V, Dalpiaz O, Alrabi N, Novara G, Galfano A, and Artibani W (2005). Correlation between clinical and pathological staging in a series of radical cystectomies for bladder carcinoma. *BJU Int* **95**, 786–790.
[7] Mehrsai A, Mansoori D, Taheri Mahmoudi M, Sina A, Seraji A, and Pourmand GH (2004). A comparison between clinical and pathologic staging in patients with bladder cancer. *Urol J* **1**, 85–89.
[8] Takeuchi M, Sasaki S, Ito M, Okada S, Takahashi S, Kawai T, Suzuki K, Oshima H, Hara M, and Shibamoto Y (2009). Urinary bladder cancer: diffusion--weighted MR imaging—accuracy for diagnosing T stage and estimating histologic grade. *Radiology* **251**, 112–121.
[9] El-Assmy A, Abou-El-Ghar ME, Mosbah A, El-Nahas AR, Refaie HF, Hekal IA, El-Diasty T, and Ibrahiem el H (2009). Bladder tumour staging: comparison of diffusion- and T2-weighted MR imaging. *Eur Radiol* **19**, 1575–1581.
[10] Thoeny HC, Forstner R, and De Keyzer F (2012). Genitourinary applications of diffusion-weighted MR imaging in the pelvis. *Radiology* **263**, 326–342.
[11] Rosenkrantz AB, Mussi TC, Melamed J, Taneja SS, and Huang WC (2012). Bladder cancer: utility of MRI in detection of occult muscle-invasive disease. *Acta Radiol* **53**, 695–699.
[12] Wang HJ, Pui MH, Guo Y, Yang D, Pan BT, and Zhou XH (2014). Diffusion-weighted MRI in bladder carcinoma: the differentiation between tumor recurrence and benign changes after resection. *Abdom Imaging* **39**, 135–141.
[13] Avcu S, Koseoglu MN, Ceylan K, Bulut MD, and Unal O (2011). The value of diffusion-weighted MRI in the diagnosis of malignant and benign urinary bladder lesions. *Br J Radiol* **84**, 875–882.
[14] Kobayashi S, Koga F, Kajino K, Yoshita S, Ishii C, Tanaka H, Saito K, Masuda H, Fujii Y, and Yamada T, et al (2014). Apparent diffusion coefficient value reflects invasive and proliferative potential of bladder cancer. *J Magn Reson Imaging* **39**, 172–178.
[15] Zhou G, Chen X, Zhang J, Zhu J, Zong G, and Wang Z (2014). Contrast-enhanced dynamic and diffusion-weighted MR imaging at 3.0 T to assess aggressiveness of bladder cancer. *Eur J Radiol* **83**, 2013–2018.
[16] Sevcenco S, Haitel A, Ponhold L, Susani M, Fajkovic H, Shariat SF, Hiess M, Spick C, Szarvas T, and Baltzer PA (2014). Quantitative apparent diffusion coefficient measurements obtained by 3-tesla MRI are correlated with biomarkers of bladder cancer proliferative activity. *PLoS One* **9**, e106866.
[17] Rosenkrantz AB, Obele C, Rusinek H, Balar AV, Huang WC, Deng FM, and Ream JM (2015). Whole-lesion diffusion metrics for assessment of bladder cancer aggressiveness. *Abdom Imaging* **40**, 327–332
[18] Sevcenco S, Ponhold L, Heinz-Peer G, Fajkovic H, Haitel A, Susani M, Shariat SF, Szarvas T, and Baltzer PA (2014). Prospective evaluation of diffusion-weighted MRI of the bladder as a biomarker for prediction of bladder cancer aggressiveness. *Urol Oncol* **32**, 1166–1171
[19] Takeuchi M, Sasaki S, Naiki T, Kawai N, Kohri K, Hara M, and Shibamoto Y (2013). MR imaging of urinary bladder cancer for T-staging: a review and a pictorial essay of diffusion-weighted imaging. *J Magn Reson Imaging* **38**, 1299–1309.
[20] Yoshida S, Koga F, Masuda H, Fujii Y, and Kihara K (2014). Role of diffusion-weighted magnetic resonance imaging as an imaging biomarker of urothelial carcinoma. *Int J Urol* **21**, 1190–1200
[21] Yoshida S, Koga F, Kobayashi S, Tanaka H, Satoh S, Fujii Y, and Kihara K (2014). Diffusion-weighted magnetic resonance imaging in management of bladder cancer, particularly with multimodal bladder-sparing strategy. *World J Radiol* **6**, 344–354.
[22] Koh DM and Collins DJ (2007). Diffusion-weighted MRI in the body: applications and challenges in oncology. *AJR Am J Roentgenol* **188**, 1622–1635.
[23] Padhani AR, Liu G, Koh DM, Chenevert TL, Thoeny HC, Takahara T, Dzik-Jurasz A, Ross BD, Van Cauteren M, and Collins D, et al (2009). Diffusion-weighted magnetic resonance imaging as a cancer biomarker: consensus and recommendations. *Neoplasia* **11**, 102–125.
[24] Unal O, Koparan HI, Avcu S, Kalender AM, and Kisli E (2011). The diagnostic value of diffusion-weighted magnetic resonance imaging in soft tissue abscesses. *Eur J Radiol* **77**, 490–494.
[25] Matsuki M, Inada Y, Tatsugami F, Tanikake M, Narabayashi I, and Katsuoka Y (2007). Diffusion-weighted MR imaging for urinary bladder carcinoma: initial results. *Eur Radiol* **17**, 201–204.
[26] Daggulli M, Onur MR, Firdolas F, Onur R, Kocakoc E, and Orhan I (2011). Role of diffusion MRI and apparent diffusion coefficient measurement in the diagnosis, staging and pathological classification of bladder tumors. *Urol Int* **87**, 346–352.
[27] Corona-Villalobos CP, Pan L, Halappa VG, Bonekamp S, Lorenz CH, Eng J, and Kamel IR (2013). Agreement and reproducibility of apparent diffusion coefficient measurements of dual-b-value and multi-b-value diffusion-weighted magnetic resonance imaging at 1.5 tesla in phantom and in soft tissues of the abdomen. *J Comput Assist Tomogr* **37**, 46–51.
[28] Kilickesmez O, Cimilli T, Inci E, Kayhan A, Bayramoglu S, Tasdelen N, and Gurmen N (2009). Diffusion-weighted MRI of urinary bladder and prostate cancers. *Diagn Interv Radiol* **15**, 104–110.
[29] Halefoglu AM, Sen EY, Tanriverdi O, and Yilmaz F (2013). Utility of diffusion-weighted MRI in the diagnosis of bladder carcinoma. *Clin Imaging* **37**, 1077–1083.
[30] El-Assmy A, Abou-El-Ghar ME, Refaie HF, and El-Diasty T (2008). Diffusion-weighted MR imaging in diagnosis of superficial and invasive urinary bladder carcinoma: a preliminary prospective study. *Sci World J* **8**, 364–370.
[31] Suo ST, Chen XX, Fan Y, Wu LM, Yao QY, Cao MQ, Liu Q, and Xu JR (2014). Histogram analysis of apparent diffusion coefficient at 3.0 T in urinary bladder lesions: correlation with pathologic findings. *Acad Radiol* **21**, 1027–1034.
[32] Kozlowski P, Chang SD, and Goldenberg SL (2008). Diffusion-weighted MRI in prostate cancer—comparison between single-shot fast spin echo and echo planar imaging sequences. *Magn Reson Imaging* **26**, 72–76.
[33] Chenevert TL, Galban CJ, Ivancevic MK, Rohrer SE, Londy FJ, Kwee TC, Meyer CR, Johnson TD, Rehemtulla A, and Ross BD (2011). Diffusion

coefficient measurement using a temperature-controlled fluid for quality control in multicenter studies. *J Magn Reson Imaging* **34**, 983–987.
[34] Braithwaite AC, Dale BM, Boll DT, and Merkle EM (2009). Short- and midterm reproducibility of apparent diffusion coefficient measurements at 3.0-T diffusion-weighted imaging of the abdomen. *Radiology* **250**, 459–465.
[35] Jacobs MA, Ouwerkerk R, Petrowski K, and Macura KJ (2008). Diffusion-weighted imaging with apparent diffusion coefficient mapping and spectroscopy in prostate cancer. *Top Magn Reson Imaging* **19**, 261–272.
[36] Tamada T, Sone T, Toshimitsu S, Imai S, Jo Y, Yoshida K, Yamamoto A, Yamashita T, Egashira N, and Nagai K, et al (2008). Age-related and zonal anatomical changes of apparent diffusion coefficient values in normal human prostatic tissues. *J Magn Reson Imaging* **27**, 552–556.
[37] Wang HJ, Pui MH, Guo Y, Li SR, Liu MJ, Guan J, Zhang XL, and Feng Y (2014). Value of normalized apparent diffusion coefficient for estimating histological grade of vesical urothelial carcinoma. *Clin Radiol* **69**, 727–731.
[38] Wollin DA, Deng FM, Huang WC, Babb JS, and Rosenkrantz AB (2014). Conventional and diffusion-weighted MRI features in diagnosis of metastatic lymphadenopathy in bladder cancer. *Can J Urol* **21**, 7454–7459.
[39] Roy C (2012). Tumour pathology of the bladder: the role of MRI. *Diagn Interv Imaging* **93**, 297–309.
[40] Abou-El-Ghar ME, El-Assmy A, Refaie HF, and El-Diasty T (2009). Bladder cancer: diagnosis with diffusion-weighted MR imaging in patients with gross hematuria. *Radiology* **251**, 415–421.
[41] Merkle EM and Dale BM (2006). Abdominal MRI at 3.0 T: the basics revisited. *AJR Am J Roentgenol* **186**, 1524–1532.
[42] Atlas SW, DuBois P, Singer MB, and Lu D (2000). Diffusion measurements in intracranial hematomas: implications for MR imaging of acute stroke. *AJNR Am J Neuroradiol* **21**, 1190–1194.
[43] Haider MA, van der Kwast TH, Tanguay J, Evans AJ, Hashmi AT, Lockwood G, and Trachtenberg J (2007). Combined T2-weighted and diffusion-weighted MRI for localization of prostate cancer. *AJR Am J Roentgenol* **189**, 323–328.
[44] Katahira K, Takahara T, Kwee TC, Oda S, Suzuki Y, Morishita S, Kitani K, Hamada Y, Kitaoka M, and Yamashita Y (2011). Ultra-high-b-value diffusion-weighted MR imaging for the detection of prostate cancer: evaluation in 201 cases with histopathological correlation. *Eur Radiol* **21**, 188–196.
[45] Hambrock T, Futterer JJ, Huisman HJ, Hulsbergen-vandeKaa C, van Basten JP, van Oort I, Witjes JA, and Barentsz JO (2008). Thirty-two-channel coil 3 T magnetic resonance–guided biopsies of prostate tumor suspicious regions identified on multimodality 3 T magnetic resonance imaging: technique and feasibility. *Investig Radiol* **43**, 686–694.
[46] Kobayashi S, Koga F, Yoshida S, Masuda H, Ishii C, Tanaka H, Komai Y, Yokoyama M, Saito K, and Fujii Y, et al (2011). Diagnostic performance of diffusion-weighted magnetic resonance imaging in bladder cancer: potential utility of apparent diffusion coefficient values as a biomarker to predict clinical aggressiveness. *Eur Radiol* **21**, 2178–2186.
[47] Hiwatashi A, Kinoshita T, Moritani T, Wang HZ, Shrier DA, Numaguchi Y, Ekholm SE, and Westesson PL (2003). Hypointensity on diffusion-weighted MRI of the brain related to T2 shortening and susceptibility effects. *AJR Am J Roentgenol* **181**, 1705–1709.
[48] Kang BK, Na DG, Ryoo JW, Byun HS, Roh HG, and Pyeun YS (2001). Diffusion-weighted MR imaging of intracerebral hemorrhage. *Korean J Radiol* **2**, 183–191.
[49] Schaefer PW, Grant PE, and Gonzalez RG (2000). Diffusion-weighted MR imaging of the brain. *Radiology* **217**, 331–345.
[50] Begg RC (1930). The urachus: its anatomy, histology and development. *J Anat* **64**, 170–183.
[51] Ceylan K, Taken K, Gecit I, Pirincci N, Gunes M, Tanik S, and Karaman I (2010). Comparison of cystoscopy with diffusion-weighted magnetic resonance images used in the diagnosis and follow-up of patients with bladder tumors. *Asian Pac J Cancer Prev* **11**, 1001–1004.
[52] Tekes A, Kamel IR, Chan TY, Schoenberg MP, and Bluemke DA (2003). MR imaging features of non-transitional cell carcinoma of the urinary bladder with pathologic correlation. *AJR Am J Roentgenol* **180**, 779–784.
[53] Tekes A, Kamel IR, Imam K, Chan TY, Schoenberg MP, and Bluemke DA (2003). MR imaging features of transitional cell carcinoma of the urinary bladder. *AJR Am J Roentgenol* **180**, 771–777.
[54] Tekes A, Kamel IR, Szarf G, Chan TY, Schoenberg MP, and Bluemke DA (2003). Carcinosarcoma of the urinary bladder: dynamic contrast-enhanced MR imaging with clinical and pathologic correlation. *AJR Am J Roentgenol* **181**, 139–142.
[55] Watanabe H, Kanematsu M, Kondo H, Goshima S, Tsuge Y, Onozuka M, and Moriyama N (2009). Preoperative T staging of urinary bladder cancer: does diffusion-weighted MRI have supplementary value? *AJR Am J Roentgenol* **192**, 1361–1366.
[56] Wu LM, Chen XX, Xu JR, Zhang XF, Suo ST, Yao QY, Fan Y, and Hu J (2013). Clinical value of T2-weighted imaging combined with diffusion-weighted imaging in preoperative T staging of urinary bladder cancer: a large-scale, multiobserver prospective study on 3.0-T MRI. *Acad Radiol* **20**, 939–946.
[57] Saito W, Amanuma M, Tanaka J, and Heshiki A (2000). Histopathological analysis of a bladder cancer stalk observed on MRI. *Magn Reson Imaging* **18**, 411–415.
[58] Ohgiya Y, Suyama J, Sai S, Kawahara M, Takeyama N, Ohike N, Sasamori H, Munechika J, Saiki M, and Onoda Y, et al (2014). Preoperative T staging of urinary bladder cancer: efficacy of stalk detection and diagnostic performance of diffusion-weighted imaging at 3T. *Magn Reson Med Sci* **13**, 175–181.
[59] Verma S, Rajesh A, Prasad SR, Gaitonde K, Lall CG, Mouraviev V, Aeron G, Bracken RB, and Sandrasegaran K (2012). Urinary bladder cancer: role of MR imaging. *Radiographics* **32**, 371–387.
[60] Giannarini G, Petralia G, and Thoeny HC (2012). Potential and limitations of diffusion-weighted magnetic resonance imaging in kidney, prostate, and bladder cancer including pelvic lymph node staging: a critical analysis of the literature. *Eur Urol* **61**, 326–340.
[61] Papalia R, Simone G, Grasso R, Augelli R, Faiella E, Guaglianone S, Cazzato R, Del Vescovo R, Ferriero M, and Zobel B, et al (2012). Diffusion-weighted magnetic resonance imaging in patients selected for radical cystectomy: detection rate of pelvic lymph node metastases. *BJU Int* **109**, 1031–1036.
[62] Birkhauser FD, Studer UE, Froehlich JM, Triantafyllou M, Bains LJ, Petralia G, Vermathen P, Fleischmann A, and Thoeny HC (2013). Combined ultrasmall superparamagnetic particles of iron oxide-enhanced and diffusion-weighted magnetic resonance imaging facilitates detection of metastases in normal-sized pelvic lymph nodes of patients with bladder and prostate cancer. *Eur Urol* **64**, 953–960.
[63] Thoeny HC, Froehlich JM, Triantafyllou M, Huesler J, Bains LJ, Vermathen P, Fleischmann A, and Studer UE (2014). Metastases in normal-sized pelvic lymph nodes: detection with diffusion-weighted MR imaging. *Radiology* **273**, 125–135.
[64] Thoeny HC, Triantafyllou M, Birkhaeuser FD, Froehlich JM, Tshering DW, Binser T, Fleischmann A, Vermathen P, and Studer UE (2009). Combined ultrasmall superparamagnetic particles of iron oxide-enhanced and diffusion-weighted magnetic resonance imaging reliably detect pelvic lymph node metastases in normal-sized nodes of bladder and prostate cancer patients. *Eur Urol* **55**, 761–769.
[65] Zehnder P, Studer UE, Skinner EC, Dorin RP, Cai J, Roth B, Miranda G, Birkhauser F, Stein J, and Burkhard FC, et al (2011). Super extended versus extended pelvic lymph node dissection in patients undergoing radical cystectomy for bladder cancer: a comparative study. *J Urol* **186**, 1261–1268.
[66] Fleischmann A, Thalmann GN, Markwalder R, and Studer UE (2005). Extracapsular extension of pelvic lymph node metastases from urothelial carcinoma of the bladder is an independent prognostic factor. *J Clin Oncol* **23**, 2358–2365.
[67] Bader P, Burkhard FC, Markwalder R, and Studer UE (2003). Disease progression and survival of patients with positive lymph nodes after radical prostatectomy. Is there a chance of cure? *J Urol* **169**, 849–854.
[68] Schumacher MC, Burkhard FC, Thalmann GN, Fleischmann A, and Studer UE (2008). Good outcome for patients with few lymph node metastases after radical retropubic prostatectomy. *Eur Urol* **54**, 344–352.
[69] Mir N, Sohaib SA, Collins D, and Koh DM (2010). Fusion of high b-value diffusion-weighted and T2-weighted MR images improves identification of lymph nodes in the pelvis. *J Med Imaging Radiat Oncol* **54**, 358–364.
[70] Eiber M, Holzapfel K, Ganter C, Epple K, Metz S, Geinitz H, Kubler H, Gaa J, Rummeny EJ, and Beer AJ (2011). Whole-body MRI including diffusion-weighted imaging (DWI) for patients with recurring prostate cancer: technical feasibility and assessment of lesion conspicuity in DWI. *J Magn Reson Imaging* **33**, 1160–1170.
[71] Takeuchi M, Suzuki T, Sasaki S, Ito M, Hamamoto S, Kawai N, Kohri K, Hara M, and Shibamoto Y (2012). Clinicopathologic significance of high signal intensity on diffusion-weighted MR imaging in the ureter, urethra, prostate and bone of patients with bladder cancer. *Acad Radiol* **19**, 827–833.
[72] Hwang S and Panicek DM (2007). Magnetic resonance imaging of bone marrow in oncology, Part 1. *Skelet Radiol* **36**, 913–920.
[73] Padhani AR, Koh DM, and Collins DJ (2011). Whole-body diffusion-weighted MR imaging in cancer: current status and research directions. *Radiology* **261**, 700–718.

[74] Nonomura Y, Yasumoto M, Yoshimura R, Haraguchi K, Ito S, Akashi T, and Ohashi I (2001). Relationship between bone marrow cellularity and apparent diffusion coefficient. *J Magn Reson Imaging* **13**, 757–760.

[75] Wu LM, Gu HY, Zheng J, Xu X, Lin LH, Deng X, Zhang W, and Xu JR (2011). Diagnostic value of whole-body magnetic resonance imaging for bone metastases: a systematic review and meta-analysis. *J Magn Reson Imaging* **34**, 128–135.

[76] Schmidt GP, Reiser MF, and Baur-Melnyk A (2009). Whole-body MRI for the staging and follow-up of patients with metastasis. *Eur J Radiol* **70**, 393–400.

[77] Pearce T, Philip S, Brown J, Koh DM, and Burn PR (2012). Bone metastases from prostate, breast and multiple myeloma: differences in lesion conspicuity at short-tau inversion recovery and diffusion-weighted MRI. *Br J Radiol* **85**, 1102–1106.

[78] Padhani AR and Gogbashian A (2011). Bony metastases: assessing response to therapy with whole-body diffusion MRI. *Cancer Imaging* **11**(Spec No A), S129–S145.

[79] Koh DM, Blackledge M, Padhani AR, Takahara T, Kwee TC, Leach MO, and Collins DJ (2012). Whole-body diffusion-weighted MRI: tips, tricks, and pitfalls. *AJR Am J Roentgenol* **199**, 252–262.

[80] Khoo MM, Tyler PA, Saifuddin A, and Padhani AR (2011). Diffusion-weighted imaging (DWI) in musculoskeletal MRI: a critical review. *Skelet Radiol* **40**, 665–681.

[81] Wang T, Wu X, Cui Y, Chu C, Ren G, and Li W (2014). Role of apparent diffusion coefficients with diffusion-weighted magnetic resonance imaging in differentiating between benign and malignant bone tumors. *World J Surg Oncol* **12**, 365.

[82] Subhawong TK, Jacobs MA, and Fayad LM (2014). Diffusion-weighted MR imaging for characterizing musculoskeletal lesions. *Radiographics* **34**, 1163–1177.

[83] Mulkern RV and Schwartz RB (2003). In re: characterization of benign and metastatic vertebral compression fractures with quantitative diffusion MR imaging. *AJNR Am J Neuroradiol* **24**, 1489–1490 [author reply 1490–1481].

[84] Dietrich O, Biffar A, Reiser MF, and Baur-Melnyk A (2009). Diffusion-weighted imaging of bone marrow. *Semin Musculoskelet Radiol* **13**, 134–144.

[85] Padhani AR, van Ree K, Collins DJ, D'Sa S, and Makris A (2013). Assessing the relation between bone marrow signal intensity and apparent diffusion coefficient in diffusion-weighted MRI. *AJR Am J Roentgenol* **200**, 163–170.

[86] Hayashida Y, Hirai T, Yakushiji T, Katahira K, Shimomura O, Imuta M, Nakaura T, Utsunomiya D, Awai K, and Yamashita Y (2006). Evaluation of diffusion-weighted imaging for the differential diagnosis of poorly contrast-enhanced and T2-prolonged bone masses: initial experience. *J Magn Reson Imaging* **23**, 377–382.

[87] Biffar A, Dietrich O, Sourbron S, Duerr HR, Reiser MF, and Baur-Melnyk A (2010). Diffusion and perfusion imaging of bone marrow. *Eur J Radiol* **76**, 323–328.

[88] Funatsu H, Imamura A, Takano H, Ueda T, and Uno T (2012). Can pretreatment ADC values predict recurrence of bladder cancer after transurethral resection? *Eur J Radiol* **81**, 3115–3119.

[89] Rosenkrantz AB, Mussi TC, Spieler B, Melamed J, Taneja SS, and Huang WC (2012). High-grade bladder cancer: association of the apparent diffusion coefficient with metastatic disease: preliminary results. *J Magn Reson Imaging* **35**, 1478–1483.

[90] Yoshida S, Koga F, Kobayashi S, Ishii C, Tanaka H, Tanaka H, Komai Y, Saito K, Masuda H, and Fujii Y, et al (2012). Role of diffusion-weighted magnetic resonance imaging in predicting sensitivity to chemoradiotherapy in muscle-invasive bladder cancer. *Int J Radiat Oncol Biol Phys* **83**, e21–e27.

[91] Koga F, Yoshida S, Tatokoro M, Kawakami S, Fujii Y, Kumagai J, Neckers L, and Kihara K (2011). ErbB2 and NFkappaB overexpression as predictors of chemoradiation resistance and putative targets to overcome resistance in muscle-invasive bladder cancer. *PLoS One* **6**, e27616.

[92] Shariat SF, Tokunaga H, Zhou J, Kim J, Ayala GE, Benedict WF, and Lerner SP (2004). p53, p21, pRB, and p16 expression predict clinical outcome in cystectomy with bladder cancer. *J Clin Oncol* **22**, 1014–1024.

[93] Kruger S, Weitsch G, Buttner H, Matthiensen A, Bohmer T, Marquardt T, Sayk F, Feller AC, and Bohle A (2002). HER2 overexpression in muscle-invasive urothelial carcinoma of the bladder: prognostic implications. *Int J Cancer* **102**, 514–518.

[94] Shariat SF, Karakiewicz PI, Ashfaq R, Lerner SP, Palapattu GS, Cote RJ, Sagalowsky AI, and Lotan Y (2008). Multiple biomarkers improve prediction of bladder cancer recurrence and mortality in patients undergoing cystectomy. *Cancer* **112**, 315–325.

[95] Yoshida S, Koga F, Kawakami S, Ishii C, Tanaka H, Numao N, Sakai Y, Saito K, Masuda H, and Fujii Y, et al (2010). Initial experience of diffusion-weighted magnetic resonance imaging to assess therapeutic response to induction chemoradiotherapy against muscle-invasive bladder cancer. *Urology* **75**, 387–391.

[96] El-Assmy A, Abou-El-Ghar ME, Refaie HF, Mosbah A, and El-Diasty T (2012). Diffusion-weighted magnetic resonance imaging in follow-up of superficial urinary bladder carcinoma after transurethral resection: initial experience. *BJU Int* **110**, E622-627.